Experiments in Fluids 7, 145–156 (1989)

Experiments in Fluids

2-D transonic flow with energy supply by homogeneous condensation: Onset condition and 2-D structure of steady Laval nozzle flow *

G. Schnerr

Institut für Strömungslehre und Strömungsmaschinen, Universität (TH) Karlsruhe, Kaiserstraße 12, D-7500 Karlsruhe 1, F. R. Germany

Abstract. A generalized form of the similarity law for the condensation onset Mach number of water vapor in air in the transonic and supersonic range for water vapor flow in moist air is derived from well known basic approaches for supersonic nozzles. These statements are confirmed by extensive experimental investigations in Laval nozzles, as well as by results of other authors and computations on the basis of the Euler equation linked with the classical theory of nucleation and droplet growth. In this experimental research priority is given to the qualitative description of the two-dimensional condensation processes, and their effects in transonic flows in nozzles of different geometrical configuration (e.g. slightly or well curved). A quantitative discussion of 2-D structures in condensation regions requires the introduction of a characteristic angle along streamlines. It is then directly possible to describe the different types of compression disturbances in supersonic flows with heat addition.

List of symbols

a	exponent of the similarity law
g	condensate mass fraction $[g_{H_2O\text{-liquid}}/kg_{moist\ air}]$
p	static pressure
R	radius of the wall curvature
T	absolute temperature
x	cartesian coordinate, mixing ratio $[g_{H_2O\text{-vapor}}/kg_{dry\ air}]$
y	cartesian coordinate
α	coefficient of the similarity law, Mach angle
$\bar{\alpha}$	coefficient of the similarity law
$\bar{\bar{\alpha}}$	coefficient of the similarity law
$\tilde{\alpha}$	coefficient of the similarity law, average value
β	coefficient of the similarity law
$\tilde{\beta}$	coefficient of the similarity law, average value
δ	angle between characteristic and iso-Mach line
Δ	difference

Indices

ad	adiabatic
c	condensation onset
f	frozen
n	neutral point
s	saturation
0	stagnation condition
1	initial state
*	critical condition
–	average value
=	average value

Non-dimensional parameters

K	characteristic quantity of geometry
M	Mach number
γ	specific heat ratio
Φ	relative humidity

1 Introduction

The phase transition of rapidly expanding vapor or gas vapor mixtures is usually not observed at thermodynamic equilibrium. In the supersaturated metastable vapor phase homogeneous nucleation occurs. Then, after a characteristic adiabatic supercooling, essential condensation starts to grow. Transonic flows of moist air expand to a certain adiabatic supercooling $\Delta T_{ad} = T_s - T_c$, the difference of saturation and condensation onset temperature, which is about 50–60 K. By that, the condition for an extreme rise of homogeneous nucleation rates is fulfilled. Moreover, this supersaturation means that the latent heat can only be supplied in the supersonic range. For the first time this fundamental result was proved theoretically by Oswatitsch (1941 and 1942). In the presence of high cooling rates, the only ones to be discussed in this paper, the amount of the usually existing additional heterogeneous condensation is of no importance.

Pressure and density disturbances in the flow, caused by heat supply, can either be steady (continuous or with a shock) or unsteady (periodically oscillating). The prevention of condensation onset is of essential importance to technical applications, e.g. turbomachines. Droplets may destroy the blades. Steady or oscillating shock waves may cause operating problems or crash of bladerows due to vibrations. Homogeneous condensation is also observed in transonic flow around airfoils in free atmosphere. So far, theoretical and experimental simulation of condensation processes to be expected in cryogenic wind tunnels, have been studied in a few cases only and by means of simplified models (Hall

* This work is dedicated to my teacher of science, Professor Dr.-Ing. J. Zierep, on the occasion of his 60th birthday.

(1976, 1979a, b), Koppenwallner and Dankert (1979a, b), Wagner (1982), Wagner and Düker (1984), Wegener (1980, 1987)). Such wind tunnels operate with pure nitrogen, which is cooled down to about 100 K. Local accelerations, producing additional supercooling, e.g. around profiles, may cause condensation onset of the nitrogen. Measured data would become unusable. What is especially interesting is the dependence of the condensation onset in 2-D flows on the caracteristic parameters, e.g. the free stream Mach number, or the thickness ratio of a profile, or the angle of attack. This paper deals with fundamental gasdynamic questions related to the condensation onset, its application to other flows, and the 2-D structure in steady transonic flow fields with heat addition.

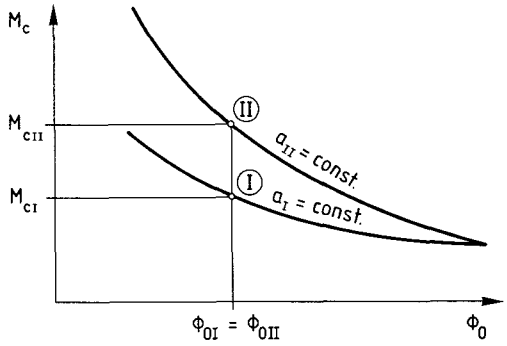

Fig. 1. Condensation onset Mach number Eq. (2) – effect of absolute temperature gradient (nozzle geometry); T_{01} = const., p_{01} = const.

2 Theory

2.1 Similarity law for the condensation onset (1-D)

The condensation process is considered in terms of gasdynamics. According to Wegener (1954) and Wegener and Mack (1958), the adiabatic supercooling is described by the empirical relationship

$$\Delta T_{ad} = f\left(\Phi_0, -\frac{dT}{dx}\right). \tag{1}$$

Equation (1) describes the relaxation process as a simple model, which is mainly dependent on thermodynamics and kinematics (geometry). Each is represented by only one quantity: the relative stagnation humidity Φ_0, and the decrease of the temperature along the streamline. Furthermore, Eq. (1) indicates that the adiabatic supercooling at fixed initial state only depends on the geometry of the flow problem.

Zierep and Lin (1967) were the first to formulate the similarity law for the Mach number at condensation onset:

$$\Phi_0^a = \frac{\frac{\gamma+1}{2}}{1+\frac{\gamma-1}{2}M_c^2}. \tag{2}$$

M_c is the onset Mach number, γ the specific heat ratio, the exponent a has to be determined by experiments. At fixed stagnation conditions, it immediately becomes apparent that a is a characteristic geometric quantity. Figure (1) shows the condensation Mach number for two values a_I, a_{II}, where $a_I < a_{II}$. The nozzle with the higher relaxation (higher condensation onset Mach number) is related to the higher value of a.

Zierep and Lin (1967) make the following empirical approach to determine the exponent a:

$$a = \alpha \cdot K^\beta = \alpha \left\{ \frac{\gamma+1}{2(\gamma-1)} \left(-\frac{d\left(\frac{T}{T_{01}}\right)}{d\left(\frac{x}{y^*}\right)} \right)^* \right\}^\beta. \tag{3}$$

T_{01} is the stagnation temperature, and $2y^*$ the total nozzle height at the throat. The constants α and β are determined experimentally: $\alpha = 0.208$ and $\beta = 0.59$. Frank's (1983, 1985) investigations confirm these values in the examined range.

Contrary to Eq. (1), Eq. (3) with Eq. (2) should lead to the result that, in case of T_{01} = const., the condensation Mach numbers are equal if geometrical similarity exists, although, the decisive absolute temperature gradient $(-dT/dx)^*$ (K/cm) may differ extremely. This means, the application to other nozzles is restricted to a limited range of validity, namely $y^* \approx$ const. This fact was already pointed out by Zierep and Lin (1967). According to Frank (1985), the stationary case is established at $\Phi_0^a \approx 0.98$ and not at $M_c = 1$, resp. $\Phi_0 = 1$ (= 100%). Therefore, the temperature gradient may not fall below a lower limit.

In the following, the approach given by Eq. (3) is generalized, and a correlation between a and $(-dT/dx)^*$ is deduced. The absolute temperature gradient mentioned above is split up as follows:

$$a = \bar{\alpha}\left(\frac{y^*}{T_{01}}\right)^\beta \left(-\frac{dT}{dx}\right)^{*\beta} \tag{4}$$

$$\bar{\alpha} = \alpha\left(\frac{\gamma+1}{2(\gamma-1)}\right)^\beta. \tag{5}$$

A correlation exists between a and the absolute temperature gradient if

$$\beta = \text{const. and } \bar{\alpha} = \bar{\alpha}\left(\frac{y^*}{T_{01}}\right)^\beta = \text{const.} \tag{6}$$

so that

$$a = \bar{\alpha}\left(-\frac{dT}{dx}\right)^{*\beta}. \tag{7}$$

In the relaxation area, the gradient at critical state is always inserted as an average value. The coefficient α, which has been considered constant before, now changes with respect to the characteristic length. Within the given conditions, this similarity law is no longer restricted to nozzle flows. Besides y^* a profile length can immediately be used in Eq. (4)

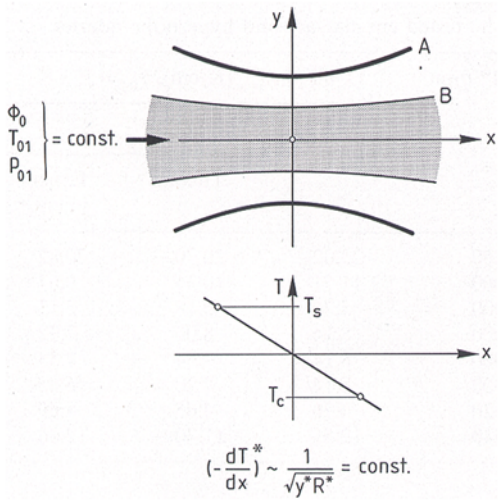

Fig. 2. Equivalent nozzles with identical time scale along the axis (1-D); $\Phi_0 = \text{const.}$, $T_{01} = \text{const.}$, $p_{01} = \text{const.}$; $(-dT^*/dx) \sim 1/\sqrt{y^* R^*} = \text{const.}$

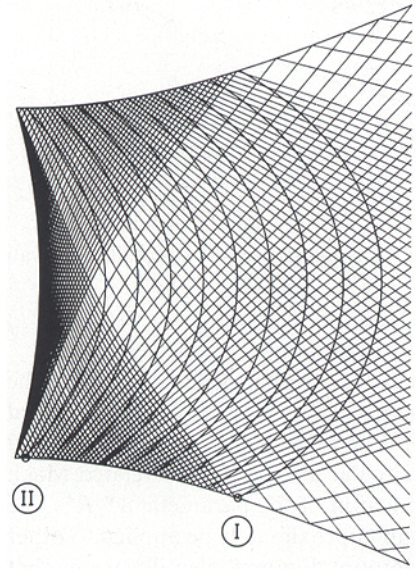

Fig. 3. Isentropic flow in a hyperbolic nozzle – characteristics and iso-Mach lines

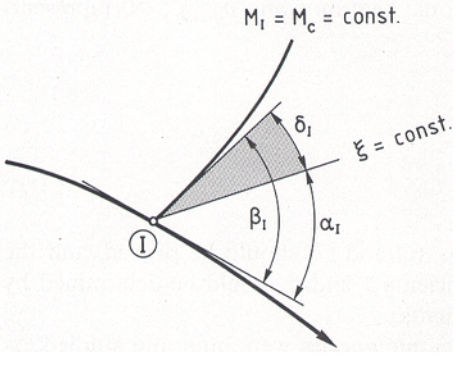

Fig. 4. Characteristic angles α, β, δ at wall point I, supersonic heating front

(Schnerr 1986). The internal streamline B belongs to the streamline A along the wall (Fig. 2). Both possible nozzles, with this pair of streamlines, have the identical temperature gradient $(-dT/dx)^* \sim 1/\sqrt{(y^* \cdot R^*)}$ in the plane of symmetry. Thus, from a 1-D point of view, a fixed stagnation condition indicates the same condensation temperature T_c or onset Mach number M_c. This is the content of the Eqs. (2) and (7).

2.2 2-D effects in isentropic Laval nozzle flow

The similarity law as discussed before is based on a 1-D model. 2-D effects, essential for the condensation process, are shown in Fig. 3. Besides the computed grid of isentropic characteristics some iso-Mach lines are plotted. The boundary on the left of the calculation range is the vertex line (normal velocity component $v=0$). In a supersonic nozzle, a certain condensation onset Mach number is always reached first at the wall. At the point on the wall where condensation starts, two angles are important: the Mach angle α between ascending characteristic ξ and tangent to the wall, as well as the angle β between the isentropic iso-Mach line and the tangent to the wall (Fig. 4). The angular difference is defined as

$$\delta = \beta - \alpha \tag{8}$$

With heat supply, the characteristic angle δ is of great importance to the development of the condensation front. The first case to be analyzed is $\delta > 0$ (Fig. 3, position I). There, the characteristics are inclined downstream of the iso-Mach line, determined by the wall point I. They do not interact with the front $M = \text{const.}$ If the iso-Mach line under consideration is a condensation onset front, the pressure increases downstream of this front as a result of heat release. Simultaneously the local Mach number decreases, which means that α becomes larger and the characteristic angle δ smaller. When the heat release, i.e. condensate mass fraction g, is high enough, δ becomes negative. As a consequence the pressure disturbances, caused by the condensation process, intersect the initial onset front $M_c = \text{const.}$ Consequently the relaxation increases.

If $\delta < 0$ is already given in the isentropic flow (Fig. 3, position II), this interaction may totally alter the flow structure. This process is well reproduced by Bartlmä's (1966) calculation of characteristics considering supersonic nozzle flow with relaxation. Figure 5 and 6 show the results for the angles α, β, δ along the nozzle wall. The nozzles 4 and 6 (Table 1) represent the limits of the investigated wall curvatures $0.0375 \leqq y^*/R^* \leqq 0.6$. In the transonic condensation range δ is mainly positive in the slightly curved nozzle 4, negative, however, in the well curved nozzle 6. According to Table 1, both nozzles show about the same absolute temperature gradient in the plane of symmetry. This means that nozzles with equal cooling rates are likely to create very different 2-D homogeneous condensation processes.

Position $\delta = 0$ is of particular interest. Heat supply may influence the condensation front upstream of this point,

Table 1. Theoretically and experimentally determined critical temperature gradients of the tested circular arc and hyperbolic nozzles

Nozzle		y^* (mm)	R^* (mm)	y^*/R^*	$y^* R^*$ (mm^2)	$(-dT/dx)^*_{axis}$ (K/cm), $T_{01}=293$ K		
						1-D	2-D	
							Theory	Experiment
1	Bartlmä (1966)	15	50	0.3000	750	23.02	20.70	20.82
2	Bartlmä (1966)	30	100	0.3000	3 000	11.51	10.35	9.67
3	Bartlmä (1966)	60	200	0.3000	12 000	5.76	5.18	5.13
4		15	400	0.0375	6 000	8.14	8.00	7.92
5	Barschdorff (1967)	30	200	0.1500	6 000	8.14	7.64	7.33
6		60	100	0.6000	6 000	8.14	7.20	6.85
7	Barschdorff (1967)	30	584	0.0514	17 520	4.76	4.65	4.69
8	Wegener and Pouring I (1964)	20	127	0.1575	2 540	12.51	11.70	12.06

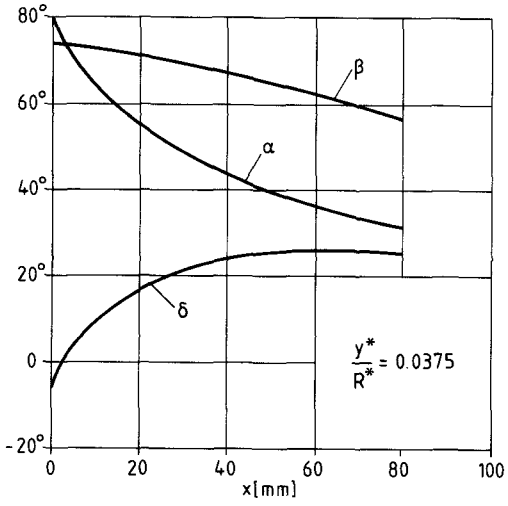

Fig. 5. Nozzle 4 – calculated characteristic angles α, β, δ along the nozzle wall

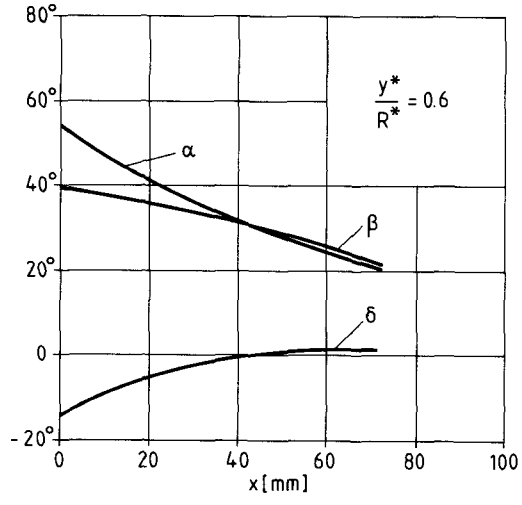

Fig. 6. Nozzle 6 – calculated characteristic angles α, β, δ along the nozzle wall

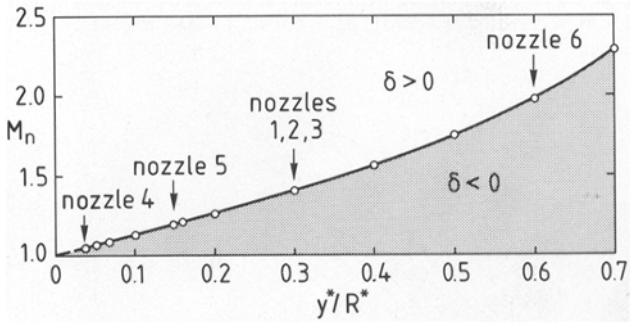

Fig. 7. Limiting curve for $\delta=0$ (isentropic flow) and different wall curvatures of circular arc nozzles

which therefore is called the isentropic neutral point. The Prandtl-Meyer expansion yields $\delta\equiv 0$, so that undisturbed condensation onset fronts, in principle, may not be expected in this type of flow. In circular arc nozzles the related Mach number M_n is only a function of the parameter y^*/R^*. The result shown in Fig. 7 can approximately be applied to other steadily curved wall contours. Figure 7 also illustrates that the theoretical limit to nearly undisturbed transonic condensation fronts is expected for $y^*/R^*\approx 0.3$. The result above can also be expressed as follows: in case of $\delta_{diabatic}>0$, the iso-Mach line $M_c=$const. is a supersonic heating front, if $\delta_{diabatic}<0$, a subsonic heating front, $\delta_{diabatic}=0$ represents sonic fronts.

3 Experiments

3.1 Test program

The validity of Eqs. (6) and (7) should be proved, and the values of the coefficients $\bar{\alpha}$ and β should be determined by systematic experiments.

In total, 6 supersonic nozzles were built and studied experimentally. Two groups were formed, each containing 3 nozzles with the same characteristics (Table 2). In the first

Table 2. Different laval nozzle types of the test series

	Nozzle	
	$y^*/R^* = \text{const.}$	$1/\sqrt{y^* R^*} = \text{const.}$
$y^* = 15$ mm = const.	1	4
$y^* = 30$ mm = const.	2	5
$y^* = 60$ mm = const.	3	6

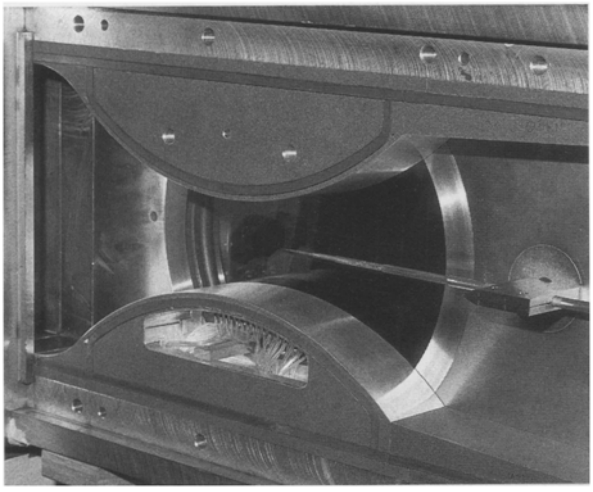

Fig. 8. Test section with circular arc nozzle No. 5, throat height $2y^* = 60$ mm, flow direction from left to right

group (nozzle 1, 2, 3) the ratio $y^*/R^* = \text{const.}$, i.e. geometrical similarity does exist. These are hyperbolic nozzles, which Bartlmä (1966) had already studied theoretically. The second group consists of 3 circular arc nozzles. Now $y^* \cdot R^* = \text{const.}$ This means that, according to Wegener (1964), the characteristic length of the critical temperature gradient (1-D) of a nozzle, $l = \sqrt{(y^* \cdot R^*)}$, is constant,

$$\left(-\frac{dT}{dx}\right)^* = 2\frac{\gamma-1}{\gamma+1} T_{01} \sqrt{\frac{1}{\gamma+1}\frac{1}{y^* \cdot R^*}} \text{ (K/cm)} \qquad (9)$$

Consequently geometrical similarity and constant absolute temperature gradient exclude each other. Table 1 gives a summary of all investigated nozzles.

3.2 Wind tunnel

The experiments were performed in the intermittant supersonic wind tunnel at the Institut für Strömungslehre und Strömungsmaschinen, Universität (TH) Karlsruhe. Figure 8 shows the opened test section, flow direction from left to right. The height of the critical cross section of the circular arc nozzle is $2y^* = 60$ mm, the tunnel width 50 mm, the radius of wall curvature $R^* = 200$ mm. The maximum effective height of this test section is 200 mm. Immediately before the entrance the flow is extremely accelerated in 2 inlet nozzles following one after another. Thus, in all approximations the boundary layer thickness may be neglected at the entry of the test section. If diabatic experiments are performed, air is directly sucked in from the atmosphere through a short pipe. The vacuum tanks (34 m^3) allow about 10–30 s blowing time of steady flow.

3.3 Methods of measurements

Flows in the test section were made visible by means of schlieren techniques and photographed with exposure times of $t = 1/125$ s ("long-time exposure") and $t = 10^{-6}$ s with a sparc light source Strobokin (Impulsphysik, Hamburg). A mercury manometer array was used for pressure measurements. Data were recorded of the pressure loss at the intake, the static pressure distribution in the whole test section as well as in the plane of symmetry of the nozzles along one tunnel sidewall. In the experiments with moist air, the relative humidity Φ_0 and the stagnation temperature in the atmosphere were measured. The pressure loss in the suction pipe (about 4 m long and 0.5 m in diameter) was always less than 0.2% of the atmospheric pressure. Changes in the state of humidity due to this influence may totally be ignored. The relative humidity at stagnation was determined with two independent measuring instruments: an aspiration psychrometer by Aßmann (Lambrecht, Göttingen), and a capacitive thin layer sensor HMP 31 UT (Vaisala OY, Helsinki). Due to the low response of the aspiration psychrometer only average values of temperatures (that is relative humidity) are measured during the test. With the fast reacting thin layer sensor changes in relative humidity are recorded on a plotter. The difference, shown between the two systems, is less than 2% relative humidity. The atmospheric pressure was determined with a mercury barometer (Lambrecht, Göttingen), the pressure loss in the intake with a pitot probe, and the stagnation temperature with a mercury thermometer. The condensation onset in nozzles was quantitatively analyzed by means of 1:1 prints and negative projections from the schlieren photographs. The compression front visible all over the cross section of the nozzle is compared with the calculated and plotted iso-Mach lines in and near the plane of symmetry. In this way, condensation onset is determined by interpolation. Additional measurements with half of the window replaced by a metal plate with pressure taps was used to determine the condensation onset. In comparison to interferometric methods, it becomes obvious that the schlieren technique is well suited for qualitative description of complicated 2-D compression disturbances caused by homogeneous condensation.

4 Results

4.1 Adiabatic nozzle flow

Figure 9 shows the distribution of static pressure measurements at the wall in the plane of symmetry of the hyperbolic

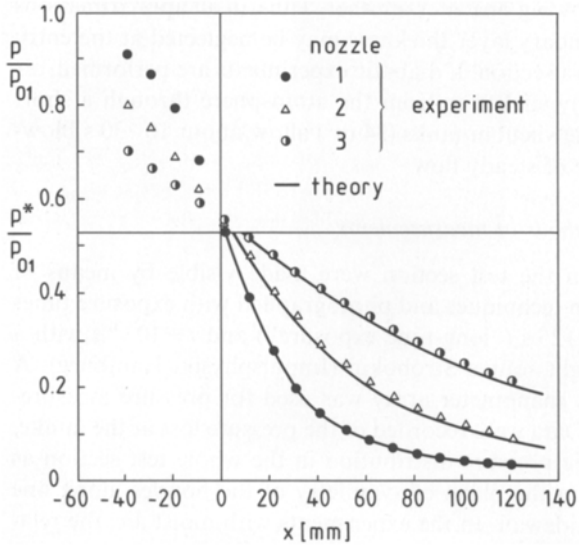

Fig. 9. Hyperbolic nozzles 1, 2, 3, – pressure distribution along the axis, adiabatic flow

nozzles 1, 2, 3. The theoretical result for the supersonic range is obtained from an isentropic calculation of characteristics. For all nozzles, theory and experiment correspond quite well. Above all this applies to the temperature gradients (Table 1, isentropic assumption in adiabatic flow). The differences in the pressure distributions due to boundary layer displacement effects are $<3\%$. This influence decreases when the wall curvature increases (higher values y^*/R^*).

4.2 Diabatic nozzle flow

According to Eq. (1) (Wegener 1954) and Eq. (2) (Zierep and Lin 1967), the influence of thermodynamics and kinematics should be discussed separately. For a given nozzle, with a constant time scale $((-dT/dx)^* = \text{const.})$, the increase of the relative humidity will cause a decrease of the condensation onset Mach number. In slender nozzles with $y^* \ll R^*$ in the limiting case of steady flow an almost normal shock extends from wall to wall. Then the flow in the supersonic range of the Laval nozzle is first reduced to subsonic speed, and then

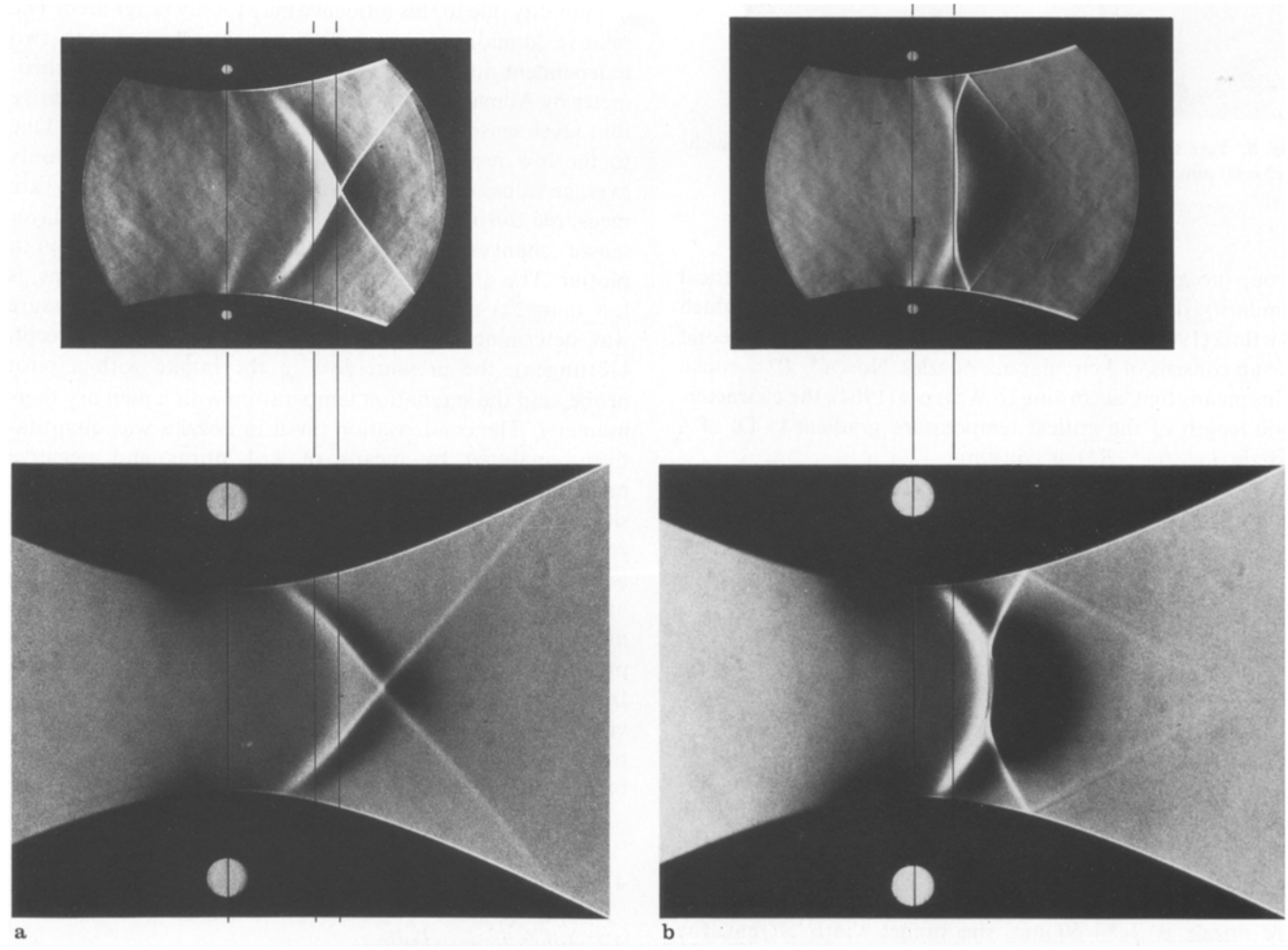

Fig. 10a and b. Effect of temperature gradient (time scale) on condensation onset in hyperbolic nozzles no. 1 (below) and no. 3 (top); **a** nozzle 3: $\Phi_0 = 29{,}2\%$, $x = 6{,}2$ g/kg, $T_{01} = 299{,}4$ K; nozzle 1: $\Phi_0 = 29{,}7\%$, $x = 7{,}3$ g/kg, $T_{01} = 301{,}8$ K; **b** nozzle 3: $\Phi_0 = 63{,}1\%$, $x = 9{,}7$ g/kg, $T_{01} = 293{,}9$ K; nozzle 1: $\Phi_0 = 63{,}6\%$, $x = 10{,}0$ g/kg, $T_{01} = 294{,}5$ K

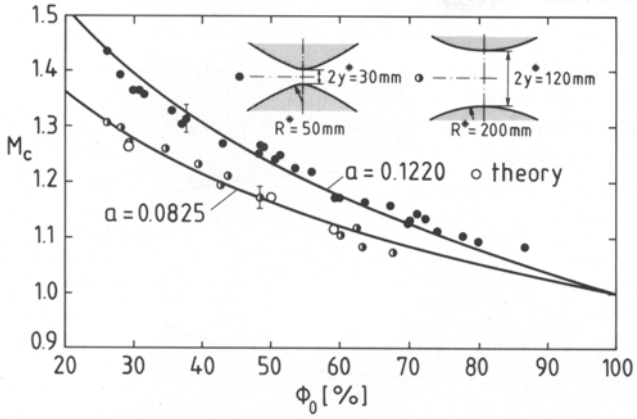

Fig. 11. Condensation onset Mach number (axis) in geometrical similar nozzles nos. 1 and 3

accelerated again to supersonic Mach numbers by means of heat supply. When Φ_0 rises further, the disturbance becomes periodically oscillating. This phenomenon was discovered by Schmidt (1962). The first similarity laws dealing with unsteady nozzle flows by homogeneous condensation were reported by Zierep and Lin (1968) and Zierep (1971, 1982). According to Figs. 5 and 7 the characteristic angle δ is always positive in nozzle 4, which means that the condensation fronts are not altered at all. M_c in the plane of symmetry is consequently well described by the 1-D model.

Figure 10a and b shows the influence of the time scale on the relaxation process for identical stagnation conditions within measuring accuracy in each case. The upper nozzle 3 ($2\,y^* = 120$ mm) is four times as large as nozzle 1 below with $2\,y^* = 30$ mm (geometrical similarity). According to Table 1, the temperature gradient $(-dT/dx)^*$ in nozzle 1 is four times as high as in nozzle 3. To explain the influence of scaling, both nozzles are illustrated such that the heights of the critical area correspond and are placed exactly one upon another. Comparing the photographs, one recognizes without any measurements that the compression disturbance in the picture below is located further downstream of the nozzle throat. There, in consequence, the condensation onset Mach number is higher. Ignoring the influence of the temperature gradient $(-dT/dx)^*$ on the condensation process, both photograph sections should be identical. This effect of the absolute temperature gradient on the condensation onset was first proved experimentally by Hermann (1942). The difference of the onset Mach numbers M_c in the investigated range is seen quantitatively in Fig. 11. The exponents a are the average values of the experiments calculated according to Eq. (2). Dohrmann (1988) supplementary computed 3 experiments in order to verify the results achieved for nozzle 3. The 2-D numerical method (Schnerr and Dohrmann 1988, 1989) is based on the Euler equation linked with the classical nucleation theory by Volmer (1939). In the droplet growth phase the surface averaged radius is used, according to Hill (1966). Theory and experiment agree quite well. The comparison of the schlieren photographs in Fig. 12 illustrates the influence of the wall curvature, when the initial conditions are nearly constant and the critical temperature gradients are identical according to the 1-D theory (Table 1, nozzle 4, 5 and 6: $y^* \cdot R^* = \text{const.}$). Decreasing radius of wall curvature implies increasing height of the nozzle throat. As a result, the characteristic "X-shock" develops more and more for increasing nozzle height at $\Phi_0 = \text{const}$. The numerical results reproduce the 2-D structure, visualized in the schlieren photographs, in all details. The agreement of the condensation onset Mach numbers expected in these 3 nozzles, is shown in Fig. 13 for $\Phi_0 < 50\%$. The measuring points encircled belong to the schlieren photographs of Fig. 12. The calculated onset Mach numbers agree well with the experimental results. This confirms the empirical approach of Eq. (7) for the similarity law. The onset in the computation is consistently defined by the heat supply, which causes without interaction ($\delta_{\text{diabatic}} = 0$) a pressure increase of ≤ 3 mbar compared to the adiabatic result. In nozzle 6 the condensation fronts for $\Phi_0 > 50\%$ are already disturbed in the plane of symmetry by compression waves extending from the walls (Fig. 14). The possibility of this behaviour in propagation of 2-D flows with condensation was already pointed out by Bratos and Meier (1976). There the onset fronts obviously are subsonic heating fronts. The intersection point of the weak inclined shock waves is now located in front of the condensation zone. This means that measurements of pressure or density in this range already deviate considerably in comparison with the adiabatic flow. This, however, should not be interpreted as condensation onset. In other words, M_c in distinctive 2-D condensation processes cannot be determined by pressure or density measurements. A correct onset condition must be defined with the condition of a minimum heat supply. In consequence it is not anymore possible to obtain a definite relation between heat supply and pressure deviation (see Figs. 17a, b). A further increase of Φ_0 results in interrupted condensation zones.

Nozzle 8 of Wegener and Pouring (1964) was used as reference for the experiments as well as for the numerical calculations on the basis of the diabatic Euler method. It was built according to the data of Wegener and Pouring (1964). Within measuring accuracy, the experimentally dermined onset Mach numbers M_c correspond quite well with the results of the authors (Fig. 15). The numerical results additionally reproduce the whole 2-D structure of the condensation zone, from the regular "X-shock" (Fig. 16, $\Phi_0 = 32\%$) to the almost normal shock (Fig. 16, $\Phi_0 = 64.8\%$). In the range of $1.132 \leq M_c \leq 1.301$ the experimental onset Mach numbers on the axis agree well with the theoretical results, and are independent of interaction ($\delta_{\text{diabatic}} > 0$) for $\Phi_0 \leq 64.8\%$. The onsets of pressure increase and heat supply are therefore identical (Fig. 17a). At nearly constant stagnation conditions in nozzle 6, the pressure disturbance already starts in front of the heat supply (Fig. 17b). In nozzle 8 the condensate mass fraction $g = 0.1\ g_{H_2O}/kg_{\text{moist air}}$ produces a pressure increase of 2.8 mbar ($\triangleq$ onset), whereas in nozzle 6 the increase is already five times higher ($\Delta p = 14.8$ mbar). In these

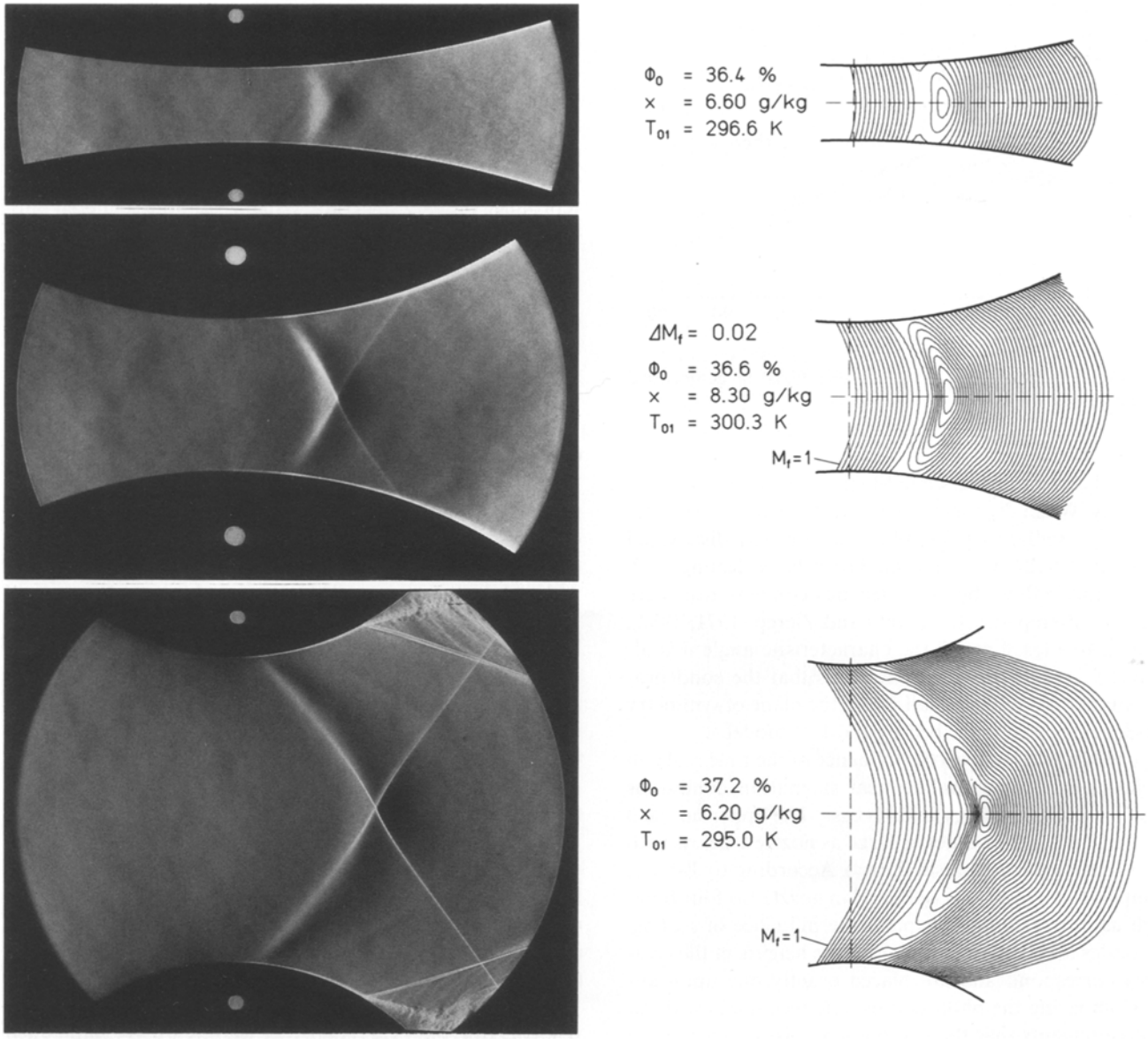

Fig. 12. Effect of wall curvature on 2-D condensation flow in circular arc nozzles nos. 4, 5, 6 with nearly the same time scale

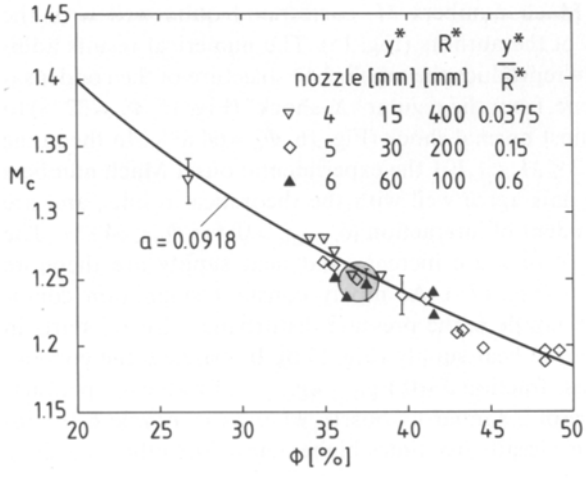

distinct 2-D processes in condensation flow, the onset Mach number M_c cannot be determined by the similarity law stated in this paper.

4.3 Determination of the coefficients $\bar{\alpha}$ and β for the condensation onset in transonic flow

According to Table 2, the nozzle experiments are analysed in three groups of constant throat heights. The experimental results of a and $(-dT/dx)^*$ are inserted in Eqs. (4) and (6), hence it follows, that the exponent β is approximately constant and $\bar{\alpha}$ changes with the throat height y^*. Eq. (6) yields

Fig. 13. Condensation onset Mach number (axis) in circular arc nozzles nos. 4, 5, 6 with nearly the same time scale

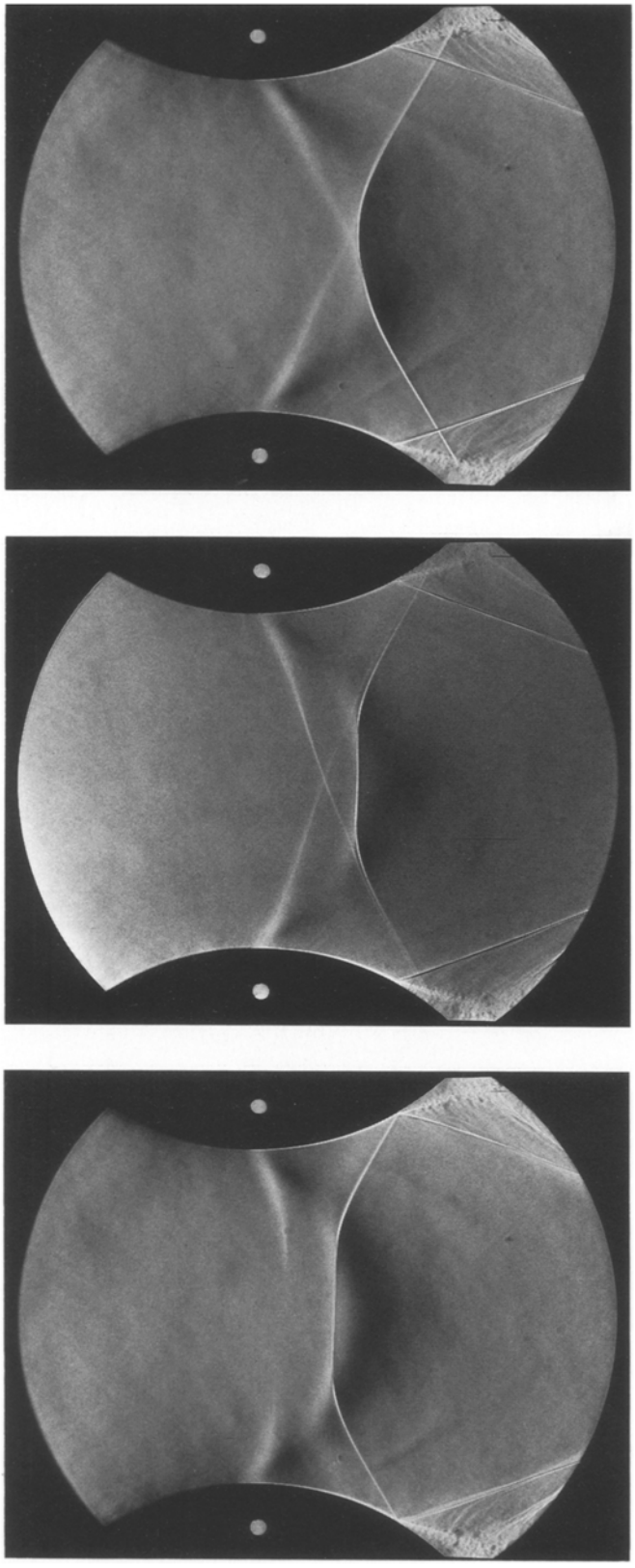

Fig. 14. Interaction of pressure waves and condensation onset in well curved nozzle no. 6; top: $\Phi_0 = 62{,}2\%$, $x = 7{,}0$ g/kg, $T_{01} = 288{,}8$ K; middle: $\Phi_0 = 63{,}2\%$, $x = 9{,}2$ g/kg, $T_{01} = 293{,}0$ K; below: $\Phi_0 = 71{,}3\%$, $x = 7{,}0$ g/kg, $T_{01} = 286{,}8$ K

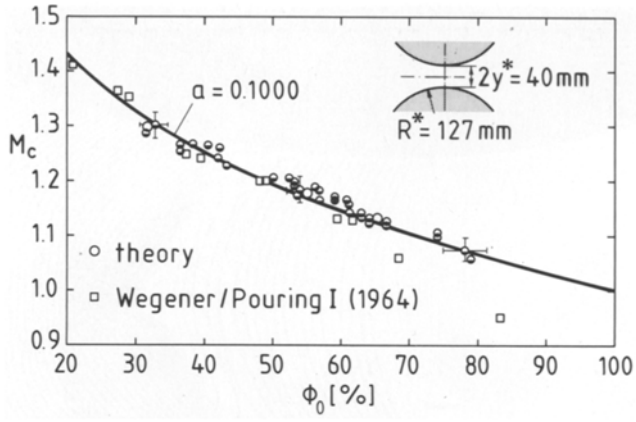

Fig. 15. Condensation onset Mach number (axis) in circular arc nozzle no. 8

Table 3. The coefficients of the similarity law for the condensation onset Eqs. (7) and (2)

y^* (cm)	$\bar{T}_0$ (K)	β	$\bar{\alpha}$ (cm/K)$^\beta$
1.5	298.55	0.2941	0.0497
3.0	298.4	0.3085	0.0494
6.0	296.85	0.3005	0.0503

$\bar{\alpha}$ constant, too, in the investigated measuring range, $T_{01} \approx$ const. (Table 3). Thus the approach of Eq. (7) is well confirmed. From Table 3 the following average values are obtained:

$$\tilde{\alpha} = 0.0498 \text{ (cm/K)}^{\tilde{\beta}} \qquad (10)$$
$$\tilde{\beta} = 0.3010.$$

Finally the similarity law for the condensation onset in transonic flows is determined, for the exponent a of Eq. (2), it follows:

$$a = 0.0498 \left(-\frac{dT}{dx} \text{(K/cm)} \right)^{* 0.3010} \qquad (11)$$

The graphic representation is shown in Fig. 18. It is verified by other experimental results, see references in Fig. 18. If the critical temperature gradient is not specified there explicitly, it was derived from the pressure distribution by means of isentropic calculation.

5 Conclusions

From the similarity law of Zierep and Lin (1967) a criterion for the onset Mach number in transonic flows with homogeneous condensation is derived, and proved by extensive experimental and theoretical investigations in supersonic nozzles. On the basis of the assumptions (local 1-D model)

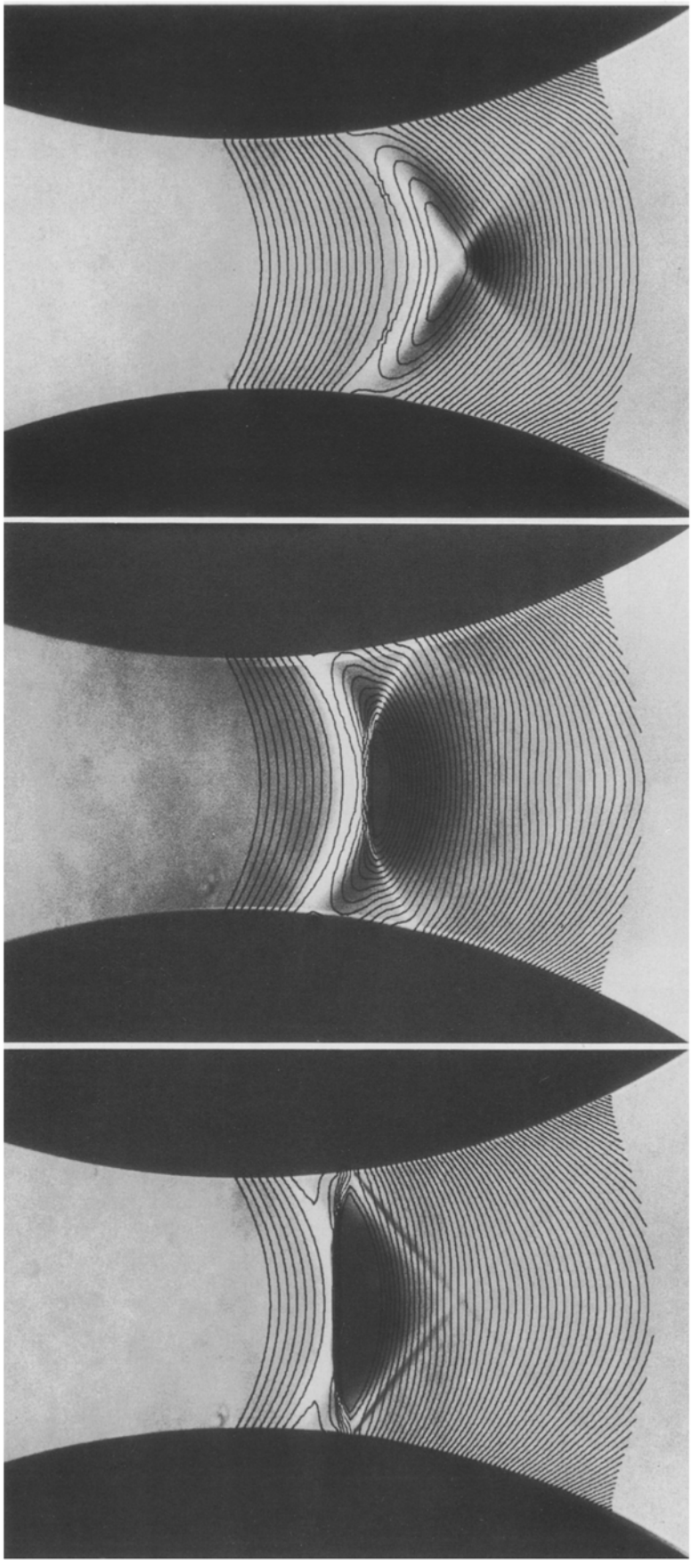

$\Phi_0 = 32.0\%$, $x = 8.43$ g/kg, $T_{01} = 302.6$ K

$\Phi_0 = 54.7\%$, $x = 9.36$ g/kg, $T_{01} = 295.6$ K

$\Phi_0 = 64.8\%$, $x = 9.08$ g/kg, $T_{01} = 292.2$ K

Fig. 16. Continuous and discontinuous flow with heat supply in nozzle 8, comparison with theory, iso-Mach lines $M_f \geq 1$, $\Delta M_f = 0.02$

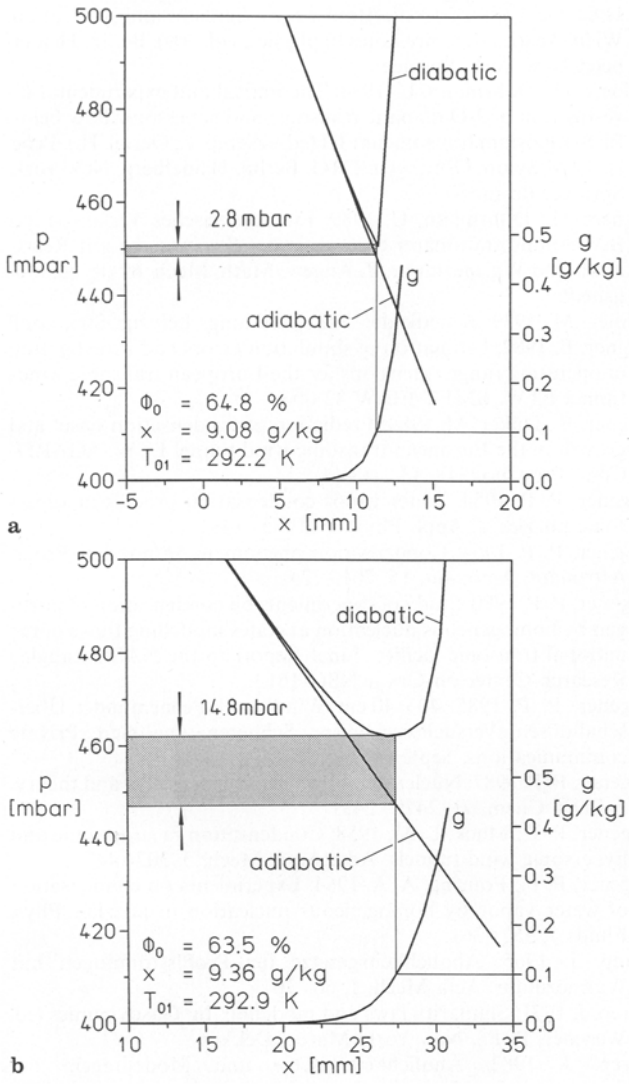

Fig. 17a and b. Condensation onset condition defined by the condensate mass fraction $g = 0.1\ g_{H_2O}/kg_{moist\ air}$, **a** nozzle 8, **b** nozzle 6 – axis

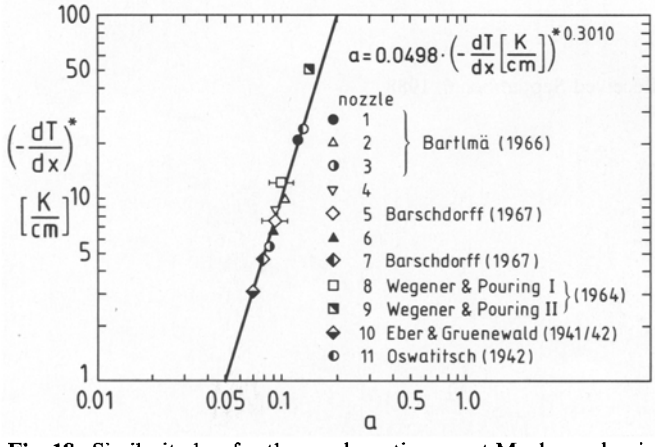

Fig. 18. Similarity law for the condensation onset Mach number in transonic flow

and boundary conditions (p_{01} and T_{01} approximately constant) of these investigations, the determining factor for the streamline considered is the critical temperature gradient. The 2-D structure of the condensation zones in supersonic nozzles can be explained immediately by the dominating curvature parameter y^*/R^*. Onset fronts are possible, which are without interaction, locally disturbed, or interrupted. Due to the interaction of the compression waves on the condensation process relaxation may increase. If the amount of the added heat is constant, the determining quantity is the characteristic angle δ of the flow without heat addition. In case of $\delta_{diabatic} > 0$, the condensation front locally is a supersonic heating front, $\delta_{diabatic} = 0$, a sonic front, and $\delta_{diabatic} < 0$ represents the subsonic heating front, e.g. diabatic Prandtl-Meyer expansions. In the transonic range of nozzles δ is only a function of y^*/R^*, and therefore applicable when geometrical similarity exists. With fixed initial conditions (Φ_0, T_{01}), the condensation process is generally dependent on (1) the absolute temperature gradient (e.g. K/cm), (2) the characteristic angle δ, (3) the amount of heat supply.

In the generalization described in this paper, the validity of the similarity law for the condensation onset is no longer restricted to nozzles. Applications to flows around profiles, e.g. to the profile surface, are directly possible. A similarity exceeding the condensation onset, e.g. for the whole transonic flow with heat supply, is not expected because of the strong interaction of flow and condensation process (Schnerr 1988). Assuming a more general function of heat distribution and considering the heat parameter $\bar{A}$, introduced by Zierep (1965) for profile flows, we obtain for Laval nozzles

$$\bar{A} \sim \frac{q}{(y^*/R^*)^{4/3}} \stackrel{!}{=} \text{const.}$$

Herein the free stream Mach number is set to one, the thickness parameter of the profile is replaced by y^*/R^* and q is the nondimensional parameter of the heat distribution. For similar transonic flows with heat supply the additional condition $\bar{A} = \text{const.}$ consequently requires higher heat supply in stronger curved nozzles.

Acknowledgements

This work was partially supported by the Deutsche Forschungsgesellschaft (DFG) and the Klein, Schanzlin & Becker Stiftung (KSB-Stiftung). I am grateful to Professor Dr.-Ing. J. Zierep for suggesting this topic and his generous support in the course of the realization of the project. For an analysis of the 1942 results of Eber and Gruenewald, Professor P. P. Wegener, Yale University, USA, made available to me unpublished, historical documents dealing with condensation in the Laval nozzles of the Peenemünde 40 × 40 cm supersonic wind tunnel. On this occasion I also want to express my thanks to him for his interest during the investigations.

References

Barschdorff, D. 1967: Kurzzeitfeuchtemessung und ihre Anwendung bei Kondensationserscheinungen in Laval-Düsen. Mitt. Inst.

Strömungslehre Strömungsmasch. Univ. (TH) Karlsruhe 6, 18–39

Bartlmä, F. 1966: Ebene Überschallströmung mit Relaxation. In: Applied Mechanics (ed. Görtler, H.), pp. 1056–1060. Proc. IUTAM Symp. München, FRG, 1964. Berlin, Heidelberg, New York: Springer

Bratos, M.; Meier, G. E. A. 1976: Two-dimensional, two-phase flows in a Laval nozzle with nonequilibrium phase transition. Arch. Mech. 28, 1025–1037

Dohrmann, U. 1988: Numerische Berechnung von 2-D Strömungen mit homogener Kondensation in Überschalldüsen. Private communication

Eber, G.; Gruenewald, K. H. 1941, 1942: Schlieren-photographs of condensation disturbances in the 40 × 40 cm Peenemünde supersonic wind tunnels. (Wegener P. P. 1985, private communication)

Frank, W. 1983: Stationäre Kondensationsvorgänge in Überschalldüsen. Forsch. Ingenieurwes. 49, 189–194

Frank, W. 1985: Condensation phenomena in supersonic nozzles. Acta Mech. 54, 135–156

Hall, R. M. 1976: Cryogenic wind tunnels – unique capabilities for the aerodynamicist. NASA Tech. Mem. X-73920

Hall, R. M. 1979 a: Onset of condensation effects as detected by total pressure probes in the Langley 0.3-meter transonic cryogenic tunnel. NASA Tech. Mem. 80072

Hall, R. M. 1979 b: Onset of condensation effects with an NACA 0012-64 airfoil tested in the Langley 0.3-meter transonic cryogenic tunnel. NASA Tech. P. 1385

Hermann, R. 1942: Der Kondensationsstoß in Überschall-Windkanaldüsen. Luftfahrtforschung 19, 201–209

Hill, Ph. G. 1966: Condensation of water vapour during supersonic expansion in nozzles. J. Fluid Mech. 25, 593–620

Koppenwallner, G.; Dankert, C. 1979 a: An experimental study of nitrogen condensation in a free jet expansion. In: Rarefied gas dynamics, 11th Symp. (ed. Campargue, R.), vol. II pp. 1107–1118. Paris: CEA

Koppenwallner, G.; Dankert, C. 1979 b: The homogeneous nitrogen condensation in expansion flows with ETW-relevant stagnation conditions. Proc. 1st. Int. Symp. Cryogenic Wind Tunnels, Southampton/UK 15.1–15.10

Oswatitsch, K. 1941: Die Nebelbildung in Windkanälen und ihr Einfluß auf Modellversuche. Jahrb. Dtsch. Luftfahrtforsch. 1, 692–703

Oswatitsch, K. 1942: Kondensationserscheinungen in Überschalldüsen. Z. Angew. Math. Mech. 22, 1–14

Schmidt, B. 1962: Beobachtungen über das Verhalten der durch Wasserdampfkondensation ausgelösten Störungen in einer Überschall-Windkanaldüse. Diss. Univ. (TH) Karlsruhe, FRG

Schnerr, G. 1986: Homogene Kondensation in stationären transsonischen Strömungen durch Lavaldüsen und um Profile. Habil. Fakultät für Maschinenbau, Univ. (TH) Karlsruhe, FRG

Schnerr, G. 1988: Homogeneous condensation in transonic flow. In: Atmospheric aerosols and nucleation (eds. Wagner, P. E.; Vali, G.). Proc. 12th Int. Conf. Atmospheric Aerosols and Nucleation, Wien, Austria (Lecture notes in physics, vol. 309). Berlin, Heidelberg, New York: Springer

Schnerr, G.; Dohrmann, U. 1988: Theoretical and experimental investigation of 2-D diabatic transonic and supersonic flow fields. In: Symposium transonicum III (eds. Zierep, J.; Oertel, H.). Proc. IUTAM Symp. Göttingen, FRG. Berlin, Heidelberg, New York: Springer (in press)

Schnerr, G.; Dohrmann, U. 1989: Ein numerisches Verfahren zur Berechnung stationärer transsonischer Strömungen mit Relaxation und Wärmezufuhr. Z. Angew. Math. Mech. 69 (to be published)

Volmer, M. 1939: Kinetik der Phasenbildung. Leipzig: Steinkopff

Wagner, B. 1982: Estimation of simulation errors and investigation of operating range extensions for the European transonic windtunnel ETW. BMFT-FB-W 82-003

Wagner, B.; Düker, M. 1984: Prediction of condensation onset and growth in the European transonic wind tunnel ETW. AGARD-Conf. Proc. no. 348, 13-1-13-11

Wegener, P. P. 1954: Water vapor condensation process in supersonic nozzles. J. Appl. Phys. 25. 1485–1491

Wegener, P. P. 1964: Condensation phenomena in nozzles. Progr. Astronaut. Aeronaut. 15, 701–724

Wegener, P. P. 1980: Study of experiments on condensation of nitrogen by homogeneous nucleation at states modelling those of the national transonic facility. Final Report to the NASA Langley Research Center on Grant NSG-1612

Wegener, P. P. 1985: 40 × 40 cm Windkanal Peenemünde: Überschalldüsen, Versuchsergebnisse, Schlierenaufnahmen. Private communications, September

Wegener, P. P. 1987: Nucleation of nitrogen: experiment and theory. J. Phys. Chem. 91, 2479–2481

Wegener, P. P.; Mack, L. M. 1958: Condensation in supersonic and hypersonic wind tunnels. Adv. Appl. Mech. 5, 307–447

Wegener, P. P.; Pouring, A. A. 1964: Experiments on condensation of water vapor by homogeneous nucleation in nozzles. Phys. Fluids 7, 352–361

Zierep, J. 1965: Ähnlichkeitsgesetze für Profilströmungen mit Wärmezufuhr. Acta Mech. 1, 60–70

Zierep, J. 1971: Similarity laws and modeling. In: Gasdynamics (ed. Wegener, P. P.). New York: Marcel Dekker

Zierep, J. 1982: Ähnlichkeitsgesetze und Modellregeln der Strömungslehre, 2nd edn. Karlsruhe: G. Braun

Zierep, J.; Lin, S. 1967: Bestimmung des Kondensationsbeginns bei der Entspannung feuchter Luft in Überschalldüsen. Forsch. Ingenieurwes. 33, 169–172

Zierep, J.; Lin, S. 1968: Ein Ähnlichkeitsgesetz für instationäre Kondensationsvorgänge in der Laval-Düse. Forsch. Ingenieurwes. 34, 97–99

Received September 6, 1988